Cerebral Cortex October 2007;17:2293–2302
doi:10.1093/cercor/bhl138
Advance Access publication December 16, 2006

Receptive Fields in Human Visual Cortex Mapped with Surface Electrodes

Daniel Yoshor[1], William H. Bosking[2], Geoffrey M. Ghose[3] and John H.R. Maunsell[2]

[1]Department of Neurosurgery, [2]Department of Neuroscience and Howard Hughes Medical Institute, Baylor College of Medicine, One Baylor Plaza, S-603, Houston, TX 77030, USA and [3]Department of Neuroscience, University of Minnesota, 6-145 Jackson Hall, 321 Church Street, Minneapolis, MN 55455, USA

Most of our understanding of the functional organization of human visual cortex comes from lesion and functional imaging studies and by extrapolation from results obtained by neuroanatomical and neurophysiological studies in nonhuman primates. Although some single-unit and field potential recordings have been made in human visual cortex, none has provided quantitative characterization of spatial receptive fields (RFs) of individual sites. Here we use subdural electrodes implanted for clinical purposes to quantitatively measure response properties in different regions of human visual cortex. We find significant differences in RF size, response latency, and response magnitude for sites in early visual areas, versus sites in later stages of both the dorsal and ventral streams. In addition, we use this technique to estimate the cortical magnification factor in early human visual cortex. The spatial and temporal resolution of cortical surface recordings suggest that this technique is well suited to examine further issues in visual processing in humans.

Keywords: electrophysiology, human, latency, magnification factor, retinotopy

Introduction

Functional magnetic resonance imaging (fMRI) and positron emission tomography allow neuroscientists to noninvasively measure changes in regional brain activity in response to visual stimuli. Functional imaging has proven to be a powerful technique for both demonstrating the presence of multiple retinotopically organized visual areas in the human brain that appear to be homologous to well-studied areas in the cortex of macaque monkey (Dougherty et al. 2003; Tootell et al. 2003; Brewer et al. 2005; Sereno and Tootell 2005), and for obtaining important clues about the types of information that are processed within these different areas. However, functional imaging only indirectly measures neuronal activity and offers limited temporal resolution compared with electrophysiological recordings. The conventional electrophysiological methods that can be used in human subjects, electroencephalography (EEG) and magnetoencephalography, offer excellent temporal resolution but lack spatial resolution. As a result, there is currently relatively little detailed information available about receptive field (RF) organization in human visual cortex. This is particularly true in later stages of visual cortex, where large RFs and less orderly topographic organization make it difficult to examine the organization of visually responsive cortex with imaging techniques.

In some patients, clinical neurosurgical approaches offer an opportunity to record directly from the human cerebral cortex. Semichronic intracranial electrodes, including penetrating depth electrodes and cortical surface subdural electrodes, implanted in epilepsy patients for clinical characterization of medically intractable seizures make it possible to conduct electrophysiological studies of human cerebral cortex in awake, behaving subjects (Engel et al. 2005).

Penetrating depth electrodes inserted in the brains of epilepsy patients for clinical purposes have been used to qualitatively describe visual responses of individual neurons in human thalamus, medial temporal cortex, and occipital cortex (Marg et al. 1968; Wilson et al. 1983). Subsequent studies have used these electrodes to systematically examine responses to visual stimuli in human hippocampal, parahippocampal, and entorhinal neurons (Fried et al. 1997; Kreiman et al. 2000, 2002; Quiroga et al. 2005). Although striking category-specific responses to visual stimuli were recorded from neurons in these areas, the long response latencies suggest that this activity may represent further cognitive processing associated with the stimulus and not a direct visual response. Clinical considerations, however, rarely result in placement of the microelectrode tip in visual cortex, so there are few opportunities to characterize responses from human visual neurons using penetrating electrodes.

Nonpenetrating electrodes implanted on the cortical surface for clinical purposes, such as subdural strip and grid arrays, offer another approach to obtaining physiological recordings directly from human visual cortex. These electrodes have been used to record local field potentials in response to visual stimuli (Noachtar et al. 1993; Arroyo et al. 1997; Schulder et al. 1999; Curatolo et al. 2000) and have provided useful data about the latency of visual responses in different regions of human visual cortex (Arroyo et al. 1997; Allison et al. 1999; Huettel et al. 2004; Gonzalez et al. 2005) and about object (Allison, Ginter et al. 1994; Allison, McCarthy et al. 1994; Allison et al. 1999) and color (Allison et al. 1993) selectivity in the ventral stream of visual processing. However, the fine spatial and temporal resolution of this recording technique has not yet been fully exploited. Here we show that surface electrodes used for clinical purposes can be used to rapidly obtain precise quantitative measures of RF size and location, response latency, and estimates of the cortical magnification factor for visual field representation in early human visual cortex.

Methods

Subjects

The Baylor College of Medicine Institutional Review Board approved all procedures used in this study. Recordings were made from patients with medically intractable epilepsy who had subdural electrodes implanted on the cortical surface of the occipital or temporal lobes for clinical purposes. Subjects included 11 males and 7 females with a mean age of 29 years (range 15–46). The patients were clinically studied in an epilepsy-monitoring unit for 4–14 days after the electrodes were implanted. Each subject had previously given informed consent and participated in one or 2 experimental sessions during this monitoring

period. Clinical monitoring continued uninterrupted during experimental sessions. Patients were screened before surgery and only those with intact visual fields and normal corrected visual acuity were included. No subject had an MRI identifiable neocortical lesion in the vicinity of the recording electrodes that were used in the experiments.

Neurophysiological Recording

Recordings were made from standard platinum clinical subdural recording electrodes embedded in silastic (AdTech, Racine, WI). The recording surface of each electrode was 2.2 mm in diameter and the centers of adjacent electrodes were separated by 10 mm. Computerized tomography scans made after electrode placement were merged with presurgical T_1-weighted magnetic resonance images (StealthStation, Medtronic, Minneapolis, MN) and the fused images were used to determine individual electrode positions relative to cortical landmarks. Electrode locations from all subjects were transferred to a common brain schematic for illustration in the figures.

Local field potentials recorded simultaneously from multiple individual subdural electrodes were amplified and filtered using a portable EEG unit (Nihon Kohden USA, Foothill Ranch, CA). Voltages from each electrode were typically referenced to a distant electrode, and bandpass filtered (0.3–120 Hz). Electrode signals were sampled at 250 Hz (16-bit resolution).

Behavioral Task

During experimental sessions, subjects were seated in their hospital bed facing a calibrated liquid crystal display video monitor (Viewsonic VP150, 1024 by 768 pixels) at a viewing distance of 57 cm, with a resulting display size of 30.5° × 22.9°. To ensure that they did not fixate the mapping stimulus (which would interfere with RF measurement), subjects were required to perform a rapid serial visual presentation (RSVP) task in which a stream of letters was presented at the center of the screen (Fig. 1). Their task was to release a button within a few hundred milliseconds after the letter "X" appeared. The time when the target letter appeared was drawn from an exponential distribution (yielding a flat hazard function) with a mean that was usually 3 s. The letters were white and were presented on a background of midlevel gray. Letters were 1° in size and were typically presented at a rate of 6 Hz but the rate of presentation was adjusted (range 2–10 Hz) to challenge the subjects and force them to fixate closely. Overall, subjects recorded 84% hits (16% standard deviation [SD]), 9% misses (9% SD), and 7% false alarms (9% SD) on the RSVP task. Only correct detection trials were used in the analysis. The fact that recording sites displayed markedly different responses from stimuli separated by as little as 1.5° (see below) shows that the RSVP task kept the subject's gaze steady throughout data collection.

Mapping Stimuli

As the subject performed the letter search task, small mapping stimuli, irrelevant to the behavioral task, were briefly flashed in different positions on the display to fill a grid over the region of interest in the visual field. The mapping stimuli consisted of small square checkerboard patterns (Fig. 1). Mapping stimuli were typically presented at a rate of 4 Hz (range 2–6 Hz) and a duty cycle of 50% (range 25–60%).

On-line displays of electrode signals were use to guide mapping. Typically, an initial mapping run with large (3°) stimuli was used to identify electrodes lying over responsive regions of visual cortex. Subsequent mapping runs with smaller (0.5–2.0°), more closely spaced stimuli were used to map RF locations and extents. In each run, stimuli were presented in 16 (4 × 4 grid) to 64 (8 × 8 grid) positions on the display monitor. For fine mapping runs we typically recorded 5–40 responses to each mapping stimulus position, and the entire run took 5–10 min to complete. In each case, the region of the visual field used for fine RF mapping was optimized for one of our electrodes but we were often able to get quantitative RF information from 2 or more electrodes during the same run.

Analysis

Analyses were performed using custom software generated for Matlab (MathWorks, Natick, MA). The first step in analysis was to exclude responses that were excessively noisy or where the voltage signal saturated. Responses that contained voltages greater than 3 SDs from the mean voltage were discarded. These exclusions removed on average only one stimulus presentation per stimulus position per electrode. All voltage responses were then filtered using a Savitzky–Golay polynomial filter ("sgolayfilt" function in Matlab, with polynomial order set to 5 and frame size set to 11, where the voltage waveforms were typically composed of 51 samples from a 200 ms time period). The filtered voltage responses were then averaged to obtain the average voltage response for each stimulus position, for each electrode (Fig. 2*A*, black line).

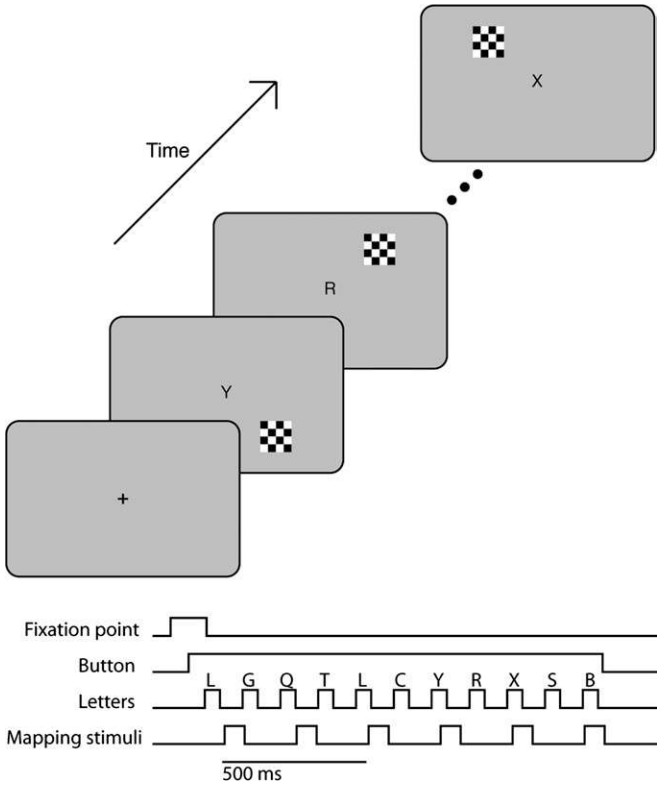

Figure 1. Letter detection task. Patients performed an RSVP letter detection task while maintaining central fixation. A fixation point appeared on the screen and subjects initiated a trial by depressing and holding a push button. After the button press, the fixation point disappeared and a series of letters was presented at the same point. Subjects responded by releasing the button when they saw the letter "X." During the RSVP task, small checkerboard mapping stimuli that were irrelevant to the task were flashed in different visual field locations to map cortical RFs.

The 99% confidence intervals for the voltage response for each stimulus position were established using a bootstrap procedure (Fig. 2*B*) (Efron 1982). Individual locations were considered to have a significant response to the stimulus if the 99% confidence intervals determined in this manner exceeded 0 V at some point during the time window 40–200 ms after the start of stimulus presentation. A time window of 40–200 ms was selected both because latencies in monkey striate and extrastriate visual cortex have typically been found to be within this range (Schmolesky et al. 1998) and because this represents roughly the amount of time available for processing between saccades in humans and monkeys. Furthermore, because visual responses were measured at a time point shorter than normal saccadic latency, it is unlikely that any saccades made toward the mapping stimulus are reflected in the recorded response, although we cannot rule out small eye movements around the fixation point.

The latency of visual responses was defined as the first 4-ms time bin in which the average voltage response deviated from the baseline voltage level by an amount equal to the 99% confidence interval (Fig. 2*B*, black vertical line). Latency calculations for each electrode were performed using a stimulus position near the center of the RF. The baseline voltage for latency calculations was obtained from the 0- to 40-ms period for that position.

To make RF maps we reduced the average voltage response for each stimulus position down to a single index of response strength. The

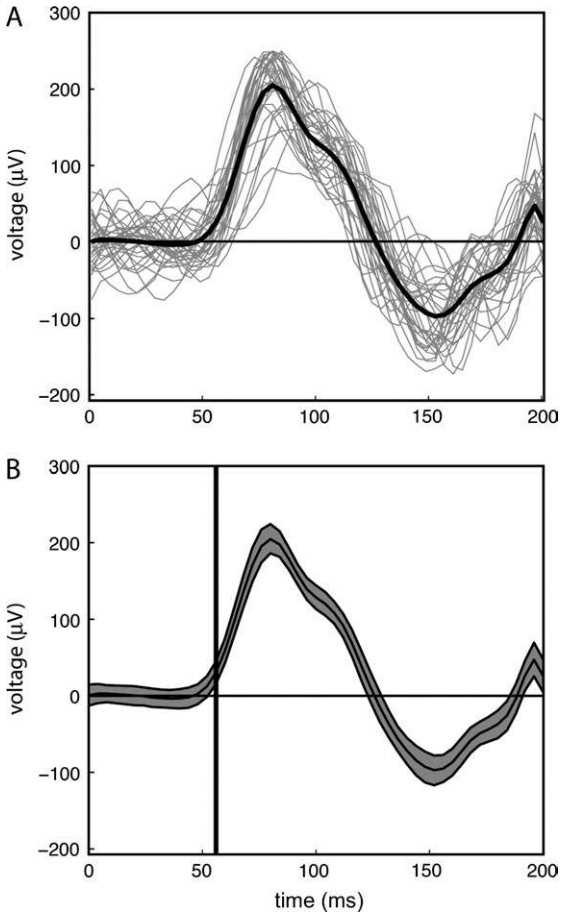

Figure 2. Processing of visual responses from single electrodes. (*A*) Filtered voltage responses from stimulus presentations for one visual field location from a single electrode (same electrode as the one illustrated in Figure 4(*A*,*B*). All voltage responses are aligned to stimulus onset. The stimulus remained on for 125 ms and evoked a consistent response from most presentations (gray curves) with waveform morphology on individual trials conforming closely to the average voltage response (black curve). (*B*) Average voltage response (black curve) and 99% confidence intervals for the average response based on a bootstrap analysis (gray shaded region). The black vertical line indicates the latency for this electrode (56 ms) calculated as the first point at which the average voltage response exceeds the baseline voltage by an amount equal to the 99% confidence interval.

index we selected was a root mean square (RMS) deviation from the mean. The baseline voltage used for the RMS calculation was the mean unstimulated voltage. This value was obtained by averaging the 0- to 40-ms time window after stimulus presentation across all stimulus positions tested. Then the RMS value for each stimulus position was then obtained by calculating the deviation at each time point in the 40- to 200-ms time range from this mean unstimulated voltage. To make RF maps, we then fit a two-dimensional Gaussian function to the RMS responses for all the sampled positions. RF width was determined by averaging the full width at half height for each of the 2 axes from the fitted Gaussian. Although we present data for RFs generated using RMS voltage as a measure of response strength, other measures, such as peak voltage obtained from each stimulus position, gave similar results.

Responses from individual electrodes were included in the RF analysis only if they met the following criteria: 1) there were 5 or more stimulus repetitions for each stimulus location, 2) there were 2 or more spatially adjacent stimulus locations that produced significant visual responses based on the bootstrap procedure described above, 3) the most responsive stimulus location was not on the border of the sampled region of visual space, and 4) at least 16 visual field locations were sampled. The RMS RF maps shown in the figures include one level of interpolation beyond the original sampling positions used in the experiment. These are used only for presentation; the quantitative analyses were performed on the original data. For several electrodes we were unable to accurately determine latency (because the interstimulus interval was too short to allow full decay of the visual response). Therefore, in the description of the results from each region of cortex, there are different numbers of electrodes for RF size and latency measurements.

Tests of statistical differences between the responses from different cortical regions were done using a one-way analysis of variance (ANOVA) (for response latencies, time to response peak, and RF width) or Kruskal–Wallis test (for response magnitudes) using a $P < 0.05$ criterion. Post hoc comparisons between particular pairs of zones were made using the "multcompare" function in Matlab with Bonferroni correction.

Results

Subjects and Recording Locations

We obtained recordings from 18 patients with electrodes implanted on the surface of visual cortex. The placement of electrodes was governed by clinical criteria. We recorded responses from between one and 6 electrodes simultaneously during RF mapping in each patient. We obtained reliable, well-localized, visual responses from 42 electrodes in 14 patients. Responsive electrode sites were found over a wide region of visual cortex including the medial wall of occipital cortex, the lateral and ventral surfaces of occipital cortex, and the posterior portion of the lingual and fusiform gyri on the ventral surface of the temporal lobe. In 3 of the 4 patients in whom we did not find electrodes with well-defined RFs, the monitored electrodes were located in the anterior portion of the parahippocampal and fusiform gyri. Thus, usable visual responses were found in 14 out of 15 patients with more posterior electrode placements.

Reliability of Responses

The responses to checkerboard stimuli at a particular location in the visual field were typically highly robust and repeatable, particularly for electrodes located in the vicinity of the occipital pole (Fig. 2). The responses in Figure 2 were based on 34 repetitions of a stimulus displayed near the center of the RF for an electrode located on the medial occipital wall just above the calcarine sulcus. The latency of the visual response at this site, defined as the time that the average voltage response first exceeded the baseline voltage level by an amount equal to the 99% confidence interval, was 56 ms.

RF Mapping

The use of rapidly presented stimuli allowed us to quickly map the spatial RF for individual recording sites. The results from a typical mapping run are illustrated in Figure 3. In this case, the electrode was located on the posterior lateral surface of occipital cortex, near the occipital pole. In Figure 3(*A*), the average response and 99% confidence intervals obtained for each mapping stimulus position are shown. Strong responses are seen from a subset of locations near 1° azimuth and –5° elevation.

Figure 3(*B*) shows the RMS voltage response at each location (see Methods for details). A 2D Gaussian function was then fit to the RMS data to estimate the RF location and dimensions (Fig. 3*C*, see Methods for details). For this site, the RF was centered at 1.3° azimuth and –5.1° elevation, and the RF width, as determined by averaging the full widths at half height for the major and minor axes from the fitted Gaussian, was 1.9°. A location near the inferior vertical meridian is consistent with

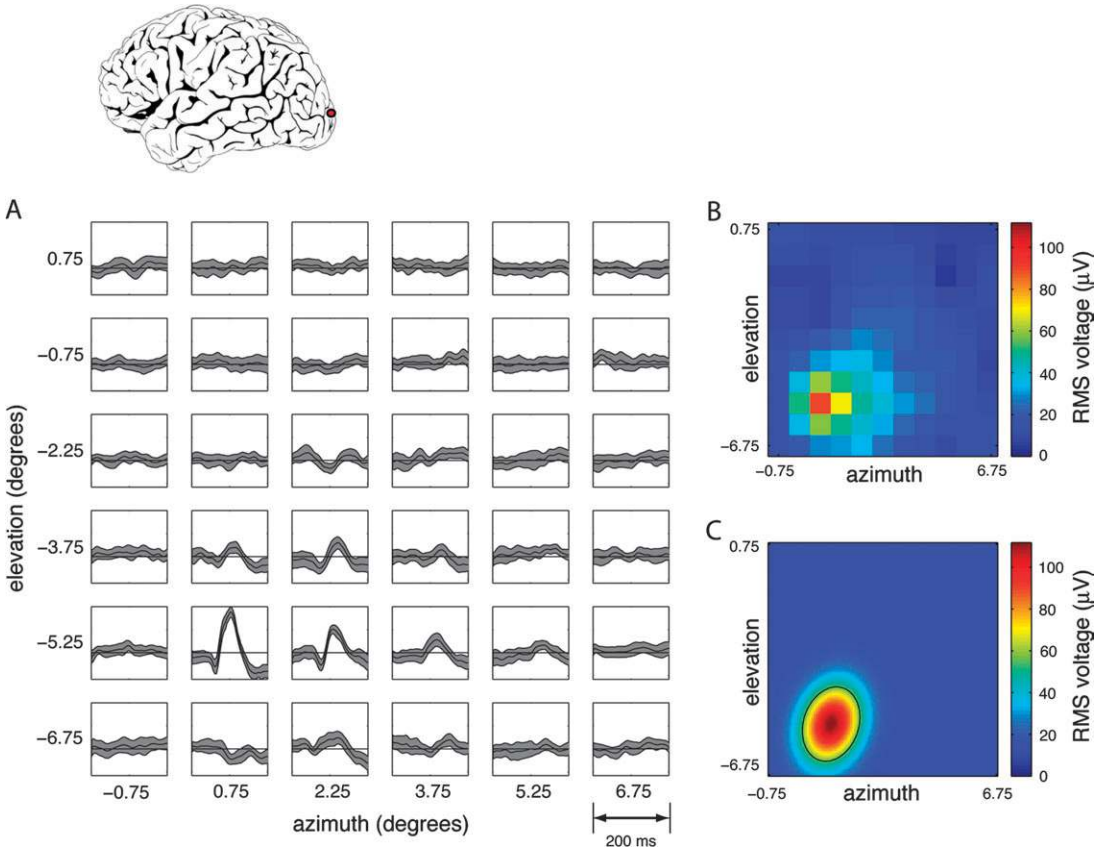

Figure 3. Quantitative characterization of RFs. (*A*) Average voltage response (black curves) and 99% confidence intervals (gray shaded regions) for each of the 36 visual field locations tested for one electrode located on the lateral surface of the occipital cortex near the occipital pole (red circle on schematic). Each panel shows the time period from 0 to 200 ms after stimulus onset. Stimulus duration was 200 ms. (*B*) RMS voltage calculated for each position using the time interval between 40 and 200 ms after stimulus onset (see Methods for details). One level of interpolation has been used for presentation of the RMS data resulting in an 11 × 11 grid rather than a 6 × 6 grid. (*C*) The best fit 2D Gaussian envelope to the data shown in panel *B*. The black ellipse indicates the half maximum response contour.

the position of the electrode, and suggests that the electrode lay near the V1/V2 border.

Analysis of Regional Variation in RF Size and Latency

We separated our recording sites into 4 broad zones that loosely correspond to different visual cortical areas as defined primarily by human fMRI studies (Fig. 5) (Van Essen and Drury 1997; Tootell et al. 2003; Grill-Spector and Malach 2004; Sereno and Tootell 2005). Functional imaging to define borders of visual cortical areas was not performed in these subjects, so the assignment of electrodes to different zones was based on coordinates and landmarks from structural MRI images. The first zone incorporates the cuneate region of cortex within approximately 2 cm of the calcarine fissure, including the most medial portion of the ventral occipital cortex and a small portion of the dorsal lateral cortex (Fig. 5, green). This region corresponds roughly to the region identified as containing V1 and V2 in humans by fMRI (Sereno et al. 1995; DeYoe et al. 1996; Dougherty et al. 2003). The second zone was defined as a strip of the dorsal lateral cortex slightly anterior to zone 1, the cuneate cortex outside of 2 cm from the calcarine, and a strip of the ventral occipital cortex more lateral to zone 1 (Fig. 5, blue). This region corresponds roughly to cortical areas V3 and V3A on the dorsal lateral surface and most dorsal portion of the cuneate and areas VP and V4v on the ventral surface (DeYoe et al. 1996; Tootell et al. 1996; Van Essen and Drury 1997; Gallant et al. 2000; Tootell and Hadjikhani 2001). The third zone was defined as a strip of cortex lateral to zone 2 (Fig. 5, yellow). This region probably contains dorsal portions of lateral occipital cortex and the human motion processing complex (MT+) (Dumoulin et al. 2000; Grill-Spector et al. 2001; Huk et al. 2002; Annese et al. 2005). The fourth zone includes the most ventral portion of lateral occipital cortex, and a region of cortex lateral and anterior to zone 2 on the ventral occipital cortex (Fig. 5, red) (Ishai et al. 2000; Haxby et al. 2001; Brewer et al. 2005; Spiridon et al. 2006). This region includes areas of visual cortex thought to respond selectively to objects and faces.

Examples of RF data obtained from electrodes located in each of the different zones are shown in Figure 4. An example, from zone 1, on the medial wall of occipital cortex, is shown in Figure 4(*A*,*B*). The RF for this site was located at 0.4° azimuth and −2.3° elevation, and the width of the RF was 0.8°. The latency of visual responses for this electrode at the center of the RF was 56 ms. Sites in this zone tended to have a short latency (Fig. 5*D*; 66 ms, SD 9) and time to peak response (Fig. 5*E*; 96 ms, SD 10) and responses in this region were significantly faster than those from zones 2 or 4. This region also had the largest peak responses (Fig. 5*F*; 267 μV, SD 231), and smallest RFs (Fig. 5*G*; 1.79°, SD 0.55).

Different electrophysiological signatures were obtained for sites located further away from the occipital pole in zone 2, such as the electrode illustrated in Figure 4(*C*,*D*). This electrode was located on the dorsal lateral surface of occipital cortex

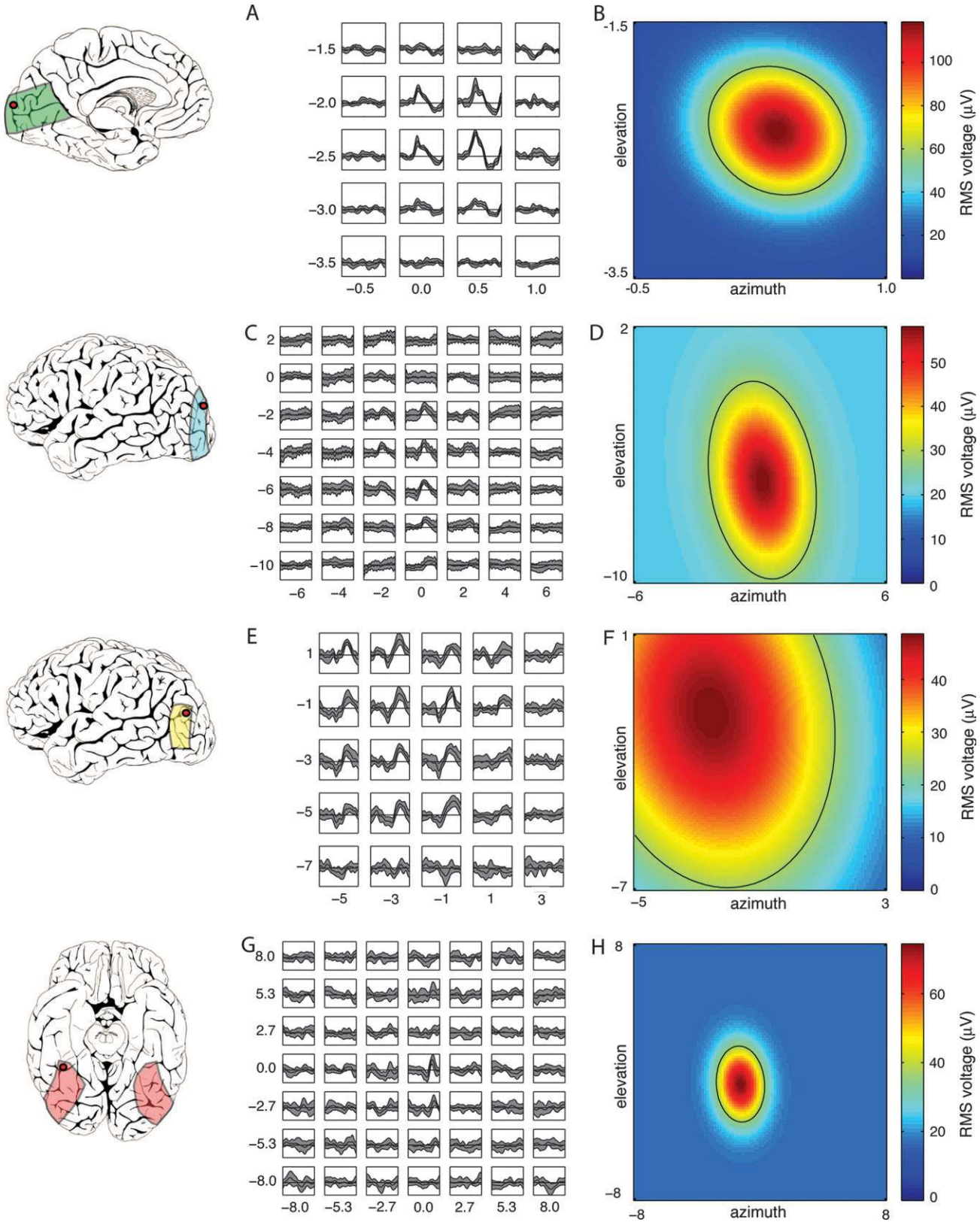

Figure 4. Examples of RFs obtained from electrodes in different parts of visual cortex. (*A*) Average voltage responses obtained from 20 visual field locations for a recording site in zone 1. The electrode (red circle, inset) was located in the cuneiform cortex approximately 1 cm from the occipital pole and 1 cm above the calcarine fissure. (*B*) The best fit Gaussian RF for the responses shown in panel *A* (color plot) and a line indicating the point at which responses were at 50% of maximum (black ellipse). (*C*) Average voltage responses obtained from 49 visual field locations for a recording site in zone 2. The electrode was located on the lateral surface of occipital cortex, well dorsal and anterior of the occipital pole. (*D*) The best fit RF for the responses shown in panel *C*. (*E*) Average voltage responses obtained from 25 visual field locations for a recording site in zone 3. The electrode was located on the lateral surface of occipital cortex, near the posterior tip of inferior temporal sulcus. (*F*) The best fit RF for the responses shown in panel *E*. (*G*) Average voltage responses obtained from 49 visual field locations for a recording site in zone 4. The electrode was located in the fusiform gyrus. (*H*) Best fit RF for the responses shown in panel *G*.

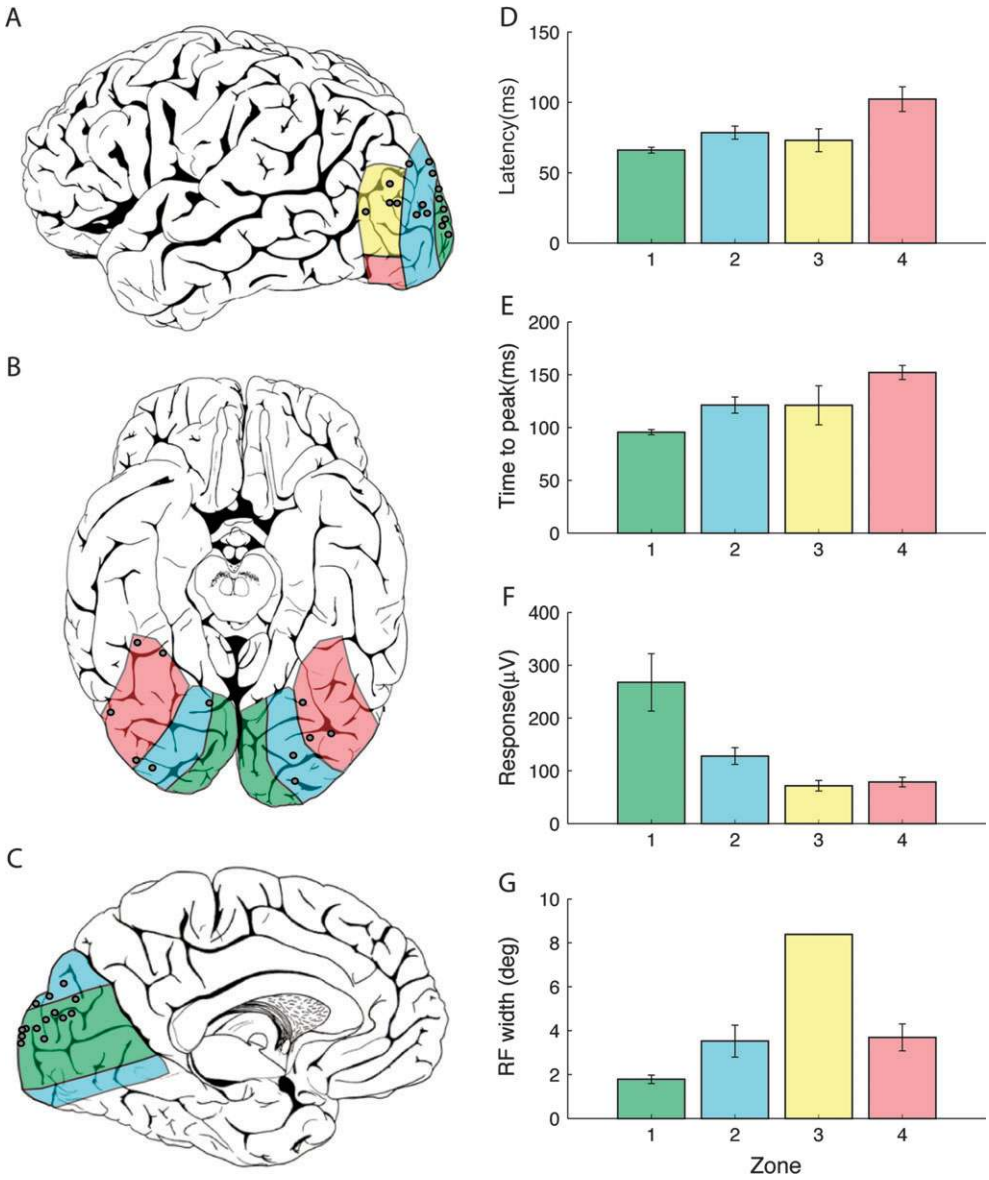

Figure 5. Summary of data obtained from each region of visual cortex. (*A*) Schematic of a lateral view of the cortex with each zone identified by a different color. The location of recording sites from all useable electrodes from all subjects has been collapsed on to this schematic using coordinates obtained from structural imaging and prominent gyral and other landmarks (gray circles). The cortex has been rotated slightly in this view so that more of the region near the occipital pole is visible. Zone 1 (green, $n = 18$) is limited to a small strip of cortex within approximately 1–2 cm of the occipital pole and should correspond approximately to the location of V1 and V2. Zone 2 (blue, $n = 13$) is formed by a strip approximately 2 cm in width lying lateral and anterior to zone 1. This zone should correspond roughly to areas V3 and V3a on the dorsal region, and areas VP and V4v on the ventral region. Zone 3 (yellow, $n = 4$) lies immediately lateral to zone 2, and should contain portions of the lateral occipital cortex, and potentially the MT complex. Zone 4 (red, $n = 7$) lies on the ventral lateral surface of the occipital cortex, and should contain areas thought to be involved in object and face processing. (*B*) Ventral view of the cortex showing zones using the same coloring scheme as in panel A. (*C*) Medial or interhemispheric view depicting the location of zones 1 and 2 in the cuneiform cortex. (*D*) Average latency for each zone. Error bars in this and remaining panels are standard error of the mean. Means for the 4 zones are significantly different by one-way ANOVA. Post hoc comparisons with Bonferroni correction show significant differences between zones 1 and 4, and between zones 2 and 4. (*E*) Average time required to reach maximum voltage for each zone. Means are significantly different by one-way ANOVA. Post hoc comparisons show significant differences between zone 1 and zone 2, zone 1 and zone 4, and zone 2 and zone 4. (*F*) Average peak voltage response obtained for each zone. Means are significantly different by Kruskal–Wallis test. Post hoc comparisons show significant differences between zone 1 and zone 3, and between zone 1 and zone 4. (*G*) Average RF size for each region. Only one RF was available for quantitative fitting for zone 3. Means are significantly different by one-way ANOVA. Post hoc comparisons with Bonferroni correction do not reach significance.

in zone 2. The RF for this site was centered at 0.1° azimuth and –5.2° elevation, and the width of this RF was 5.1°, considerably larger than what was found for sites that were closer to the occipital pole, in zone 1. The latency of the visual response for this recording site was 92 ms. Overall, sites in this region had an average latency (Fig. 5*D*; 78.5 ms, SD 16.8) and time to peak response values (Fig. 5*E*; 121.2 ms, SD 27.6) that were longer than those for zone 1 but significantly shorter than those for zone 4. Response magnitudes in this region were larger than those for zone 4 (Fig. 5*F*; 128.2 μV, SD 57.1) but RF sizes were similar (Fig. 5*G*; 3.5°, SD 1.9).

We have limited sampling from sites further lateral in zone 3. These sites tended to have larger RFs but still had short latencies. Figure 4(*E*,*F*) shows an example from this region that lies near the posterior portion of the inferior temporal sulcus. This electrode is located outside the early visual areas of

V1 through V4 and may lie at or near the typical anatomic site of the human MT+ complex (Dumoulin et al. 2000; Annese et al. 2005). This electrode responded to stimuli over a large area of the visual field (Fig. 4*E*), with an RF width of 8.4°. This RF is much larger than any found in zones 1 and 2. The latency for this site, however, was only 60 ms. Unfortunately, this is the only electrode for which we have adequate sampling to estimate RF size for this zone. Overall, sites in this region had a latency (Fig. 5*D*; 73.0 SD 16.1) and time to peak response (Fig. 5*E*; 121.0 SD 37.1) that were fast, and not statistically different from the timing of responses for zone 1 or zone 2. Response magnitudes for this region (Fig. 5*F*; 72.4 SD 21.0), however, were significantly less than those for zone 1.

An example of a recording site on the posterior fusiform gyrus in zone 4 is shown in Figure 4(*G*,*H*). This site, like several others in this region, had a small RF with reliable but long latency responses (Fig. 4*G*). The RF for this site was only 3.2°. The latency for this site of 104 ms, however, was much longer than that of sites closer to the occipital pole in zones 1 and 2. Sites in zone 4 had a much longer latency (Fig. 5*D*; 102.3, SD 23.2) and time to peak (Fig. 5*E*; 152.0, SD 17.6) than zones 1 and 2, and also had smaller response magnitudes (Fig. 5*F*; 78.7, SD 24.4). However, our mapping stimulus was always a simple checkerboard pattern. No attempt was made to optimize stimuli for different visual areas. Thus, it is possible that other stimuli might produce stronger, shorter latency responses. The average RF size for this region was only (3.7°, SD 1.4).

RF Progressions

Because electrode placement was guided by clinical concerns, we were unable to perform a detailed study of retinotopy across different visual areas in human visual cortex. However, in several cases we observed orderly progressions of RF positions across successive electrodes. An example is shown in Figure 6. In this case, a subdural electrode strip curved around the occipital pole and into the interhemispheric fissure along the medial wall of occipital cortex slightly above the calcarine fissure (Fig. 6*A*,*B*). Although we do not know the exact location of these sites relative to the V1/V2 border, we would nevertheless expect an orderly movement of RFs from near the fovea to further into the periphery of the lower visual field with movement from site 1 to site 3. Indeed, we find that the RF for the first electrode is centered at 0.8° azimuth and –0.9° elevation (Fig. 6*D*), and the RFs for the next 2 electrodes lie in more eccentric positions in the lower visual field as expected. The RF location for the second electrode is 0.8° azimuth and –2.0° elevation (Fig. 6*E*), and for the third electrode is 4.9° azimuth and –6.0° elevation (Fig. 6*F*). The movement of RF centers between the first 2 electrodes is 1.1° of over a surface distance of 1 cm in cortex. This provides an estimate of the cortical magnification factor (9.1 mm/deg) at this eccentricity (average eccentricity 1.7°).

A second example of predictable change in RF location from 2 electrodes was obtained from a recording strip placed on the lateral surface of occipital cortex near the occipital pole. In this case, the RF locations for the 2 electrodes were –0.2° azimuth and –2.1° elevation, and –0.2° azimuth and –0.4° elevation, respectively. This results in a magnification factor of 5.9 mm/deg at an average eccentricity of 1.3°. In a third case, we similarly calculated a magnification factor estimate of 5.4 mm/deg at an average eccentricity of 4.4°. The average for these 3 cases was a linear magnification factor of 6.8 mm/deg measured at an average eccentricity of 2.4°.

Discussion

Summary

We have shown that recordings from subdural electrodes implanted in human patients can provide a detailed physiological characterization of sites in visual cortex. Successful recordings were made from most of the patients tested. The data from our initial application of this technique are consistent with the maps of visual space in early human visual cortex based on lesion and fMRI studies. In addition, this technique was used to

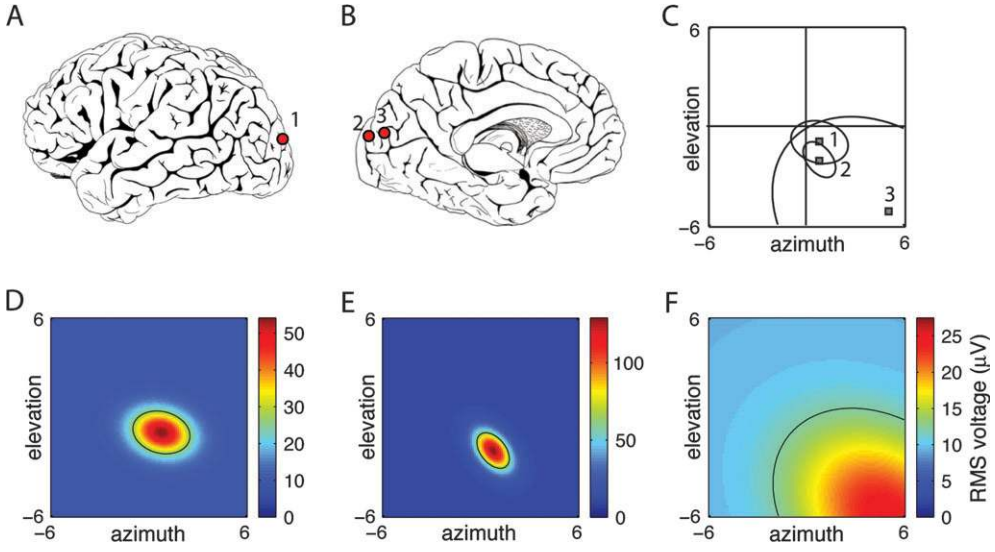

Figure 6. Orderly progression of RF location obtained from 3 electrodes on the same subdural strip. The recording strip was located on the lateral posterior surface of occipital cortex and curved around the occipital pole to enter the interhemispheric fissure. The strip is located approximately 1 cm dorsal to the level of calcarine fissure, near the V1/V2 border. (*A*) Location of recording site 1 on the strip. (*B*) Location of recording sites 2 and 3 on the strip. (*C*) The RFs of the 3 recording sites. The ellipses indicate the limits of the RF defined by the full width at half height of the Gaussian fit. The gray squares indicate the center of each RF. (*D*) The RF for the electrode at site 1 in panel *A*. (*E*) The RF for the electrode at site 2 in panel *B*. (*F*) The RF for the electrode at site 3 in panel *B*.

measure response latencies in different stages of visual cortex, and to put an upper limit on the RF size of sites in early human visual cortex. Below we consider each of these findings and discuss potential applications of this technique that could yield further insight into cortical organization.

RF Sizes in Human Visual Cortex

Our recordings represent the most direct and systematic measurements of RF sizes in early human visual cortex to date. Previous attempts to measure RF size in human visual cortex by direct physiological measures have been extremely rare. In the monkey, single-unit recordings have been employed to obtain detailed quantitative RF maps by presenting visual stimuli in different spatial locations and recording the activity elicited in visually responsive neurons but single-unit recordings in human visual cortex have been limited to qualitative descriptions of visual responses for a small number of units (Marg et al. 1968; Wilson et al. 1983). Other studies have described responses in human visual cortex using subdural (nonpenetrating) recording electrodes (Allison et al. 1993; Noachtar et al. 1993; Allison, Ginter et al. 1994; Allison, McCarthy et al. 1994; Arroyo et al. 1997; Allison et al. 1999) similar to those employed in our patients but these studies primarily focused on the category-selective nature of the responses. In most of these studies, visual stimuli were full-field or hemifield in extent, and in no case was a detailed examination of RF size and location reported. The possibility that a more systematic examination of RFs using subdural electrodes might be possible has been demonstrated in monkeys using subdural wires (Dagnelie et al. 1989) but has not been previously accomplished in humans.

Although fMRI has been very useful in determining the overall structure of the map of visual space within a visual area, it has provided limited information about the size of the RF for individual sites within each area. In 2 cases, fMRI has been used to demonstrate that later stages of visual cortex have larger RFs (Kastner et al. 2001; Smith et al. 2001) but these studies did not provide direct estimates of absolute RF size for any area. The electrophysiological recordings we obtained from surface electrodes allowed us to measure RFs directly using the same mapping stimuli employed in single-unit studies and provide novel direct and quantitative measurements of RF size in different regions of human visual cortex.

The smallest RFs that we measured in early visual cortex had a full width at half height of less than 1°. However, there are several factors that suggest that even this value overestimates the size of RFs for neurons in early visual cortex with foveal or parafoveal RFs. First, our measurements were made using electrodes with a recording area that was 2.2 mm in diameter. Although, aggregate RFs for single columns of neurons in visual cortex are not necessarily larger than the individual RFs on which they are based (Allman et al. 1985), over a distance of 2.2 mm we assume that the electrode samples from many thousands of neurons yielding an aggregate RF size that is larger than the RF size for any individual neuron. For example, based on the average magnification factors that we measured in early visual cortex, the aggregate RF sampled by a 2.2-mm electrode would be roughly 0.32° larger than the size of an individual RF. An additional factor limiting our ability to assess the size of foveal RFs was the size of the mapping stimuli that we used. The smallest RFs that we measured were obtained with a stimulus size and spacing of 0.5°. This could have contributed up to 0.5° to the final RF size that we measured. Finally, although we believe our subjects maintained good fixation on the center of the screen to perform the letter detection task, residual eye movements present during stimulus presentation could also have systematically increased our estimates of RF size. The effects of such eye movements might be reduced by monitoring eye movements and compensating for them.

Although it is not clear exactly how much each of these sources of error contribute to our current measurements, it is likely that RF sizes in early human visual cortex at parafoveal eccentricities are significantly smaller than 1° in size, and may approach 0.1° as demonstrated in the foveal representation of macaque V1 (Dow et al. 1981; Van Essen et al. 1984). Further experiments with smaller electrodes, smaller stimuli, and better control and measurement of eye position should help resolve this issue. Our current measurements should be considered an upper bound on the size of RFs in early visual cortex.

Our results also have implications for understanding the spatial resolution of subdural recording relative to other techniques. If we assume that RF sizes in early visual cortex of humans are indeed similar to those found in monkeys, then the above analysis on the effect of stimulus size and magnification factor on measured RF size implies that little spatial blurring is introduced by eye movements or oversampling of cortex by the subdural electrodes. In our study, the responses of individual electrodes appear to be based on the area immediately beneath the electrode, and individual sites respond only to a few of the mapping stimuli utilized.

Although most of our recordings were from early visual cortex, we also examined RF size for sites in later visual processing areas in both the dorsal and ventral streams. As expected, we found large RFs for sites that are further anterior on the lateral surface of visual cortex. Interestingly, we also found visually responsive sites with well-organized RFs in the ventral temporo-occipital cortex. RFs for these sites were relatively small and were largely confined to the contralateral visual field. These recording sites were found at distances of 3.5–7.0 cm from the occipital pole on the ventral surface. This places them in the vicinity of the face and object responsive regions that have been described by subdural recordings (Allison, McCarthy et al. 1994; Halgren et al. 1994; Allison et al. 1999) and fMRI (Grill-Spector and Malach 2004). However, some of our electrodes may have been in the region recently defined as the ventral occipital complex and some may have been in ventral V4 (Brewer et al. 2005). Our finding of well-defined RFs for electrodes at these locations suggests that although neurons in these regions may respond selectively to faces or other objects, they are unlikely to show complete invariance to the size and position of visual stimuli to which they are responsive (Cavonius and Hilz 1973; Rolls and Tovee 1995). We are currently investigating this issue with quantitative measurements of size and position selectivity of neurons in these and other areas measured using more complicated objects as stimuli.

Topographic Mapping and Magnification Factor

Although the spacing of the electrode arrays that we used allowed only 2–3 samples from early visual cortex to be obtained from individual patients, we found examples of RF locations and progressions that were consistent with data on human visual cortex from mapping studies based on cortical lesion and fMRI data (Van Essen 2004). Recording strips or grids with more closely spaced electrodes could likely be used for more detailed topographic mapping studies in humans.

In addition to conforming to the general layout of the map of visual space that has been established for early visual cortex, data from our recordings can also be used to provide an estimate of linear cortical magnification factor in these areas. The magnification factors we measured for early visual cortex in 3 cases yielded values (9 mm/deg at an eccentricity of 1.7°, 5.9 mm/deg at an eccentricity of 1.3°, and 5.4 mm/deg at an eccentricity of 4.4°) in the range obtained from fMRI (Sereno et al. 1995; Engel et al. 1997; Dougherty et al. 2003) and lesion studies (Horton and Hoyt 1991) of V1. Dougherty et al. (Dougherty et al. 2003) found a linear magnification factor of ~4 mm/deg at an eccentricity of 3° for V1. The subdural recording technique should be ideal for making further magnification factor estimates because the aggregate activity of multiple sites can be recorded simultaneously.

Latency of Response

Subdural electrodes offer excellent temporal resolution. The latencies measured for early visual cortex are similar to those measured in single-unit studies of monkey visual cortex (Schmolesky et al. 1998). The fastest sites had latencies under 60 ms, which is consistent with recordings from sites located in or near V1 in monkeys. Sites on the lateral or ventral surface that were slightly further from the occipital pole, which were likely in V3–V4, had latencies in the 70- to 80-ms range. Latencies on the lateral surface of occipital cortex, which could be in the region of motion sensitive regions of visual cortex in the human, showed latencies only slightly longer than found for V1. This is in accord with fast latencies found for MT and MST in the monkey (Maunsell and Van Essen 1983; Kawano et al. 1994; Maunsell 1995). Finally, in ventral cortex several centimeters anterior to the occipital pole we found much longer latencies.

The waveforms and latencies that we measured are consistent with data from several previous studies that used subdural recording electrodes (Noachtar et al. 1993; Allison, McCarthy et al. 1994; Huettel et al. 2004). However, in those studies, latencies were usually calculated on the basis of time to characteristic peaks (such as the C1, N1 and P1 waveforms) in the voltage response and not as time of the onset of the response, which is likely to be a more specific and reliable measure (but see Arroyo et al. 1997). The previous studies were often focused on using recordings from subdural electrodes to better understand the cortical generators of visual evoked potentials recorded from scalp electrodes (Noachtar et al. 1993; Allison, McCarthy et al. 1994; Arroyo et al. 1997) or the nature of the fMRI BOLD signal (Huettel et al. 2004). As a result, the potential of subdural electrodes to provide precise latency data that are valuable on their own has perhaps not been fully exploited. The exact shapes of the waveforms that we measured varied depending on the location of the recording electrode and the reference electrode. Nevertheless, the time to first significant departure of the response from baseline voltage appears to be a robust method for measuring latency, and using this method we find significant differences in latency and other response characteristics between different regions of visual cortex.

Regional Differences in Response Properties

The organization of visual cortex is often viewed as hierarchical, with progressive changes from small RFs, with simple response properties in early visual areas, to larger RF and responses governed by more complicated or abstract criteria in later processing stages (Maunsell 1995). In general, our results were consistent with this framework but there were some exceptions. Our results from the lateral occipital cortex indicate that changes in RF size and response latency are not necessarily coupled. In this region we found the largest RF, but latencies were still fairly fast, and were in fact not significantly different from those in the early visual areas (zones 1, 2; presumably V1–V4). This result is also consistent with existing data from monkey physiology experiments (Kawano et al. 1994). Zone 4 presumably contains cortical areas that are specialized for processing of objects and faces (Haxby et al. 2001; Grill-Spector and Malach 2004; Spiridon et al. 2006). We found that the RFs we measured in this region were relatively small and well defined, consistent with some recent results from single-unit recordings in monkey (DiCarlo and Maunsell 2003). Although we do not have enough data to confirm a bias in visual field coverage in these ventral areas, we found evidence of moderate size RFs with near foveal locations. Although responses to more complicated objects or faces might produce larger responses in this area, it thus seems unlikely that cells or columns of cells in this region will show complete invariance to object location or size.

Conclusions

We demonstrate that subdural electrodes can be used to measure RF size, response magnitude, and response latency for different regions in human visual cortex. This type of electrophysiological signature could be combined with data on stimulus selectivity and overall visual field mapping to better understand the number of distinct visual cortical areas that are present in humans, and the functional roles of each area. Furthermore, the spatial and temporal resolution of the technique combined with the excellent trial-to-trial repeatability suggest that subdural recordings may offer advantages over fMRI in addressing a number of important issues in visual processing in human brain such as the extent of attentional modulation, and the correlation of behavior with activity in various visual cortical areas while subjects perform visually guided tasks.

Notes

This work was supported by grants from the National Institutes of Health (K08NS045053) and The Methodist Hospital Foundation to D. Yoshor. J.H.R. Maunsell is a Howard Hughes Medical Institute Investigator.

We thank L. Rhodes, B. Pudlo, M. King, S. Pedigo, H. Tsoi, W. Morton, A. Verma, I. Goldsmith, and E. Mizrahi for assistance with intracranial recordings and M. Beauchamp and R. Grossman for helpful comments. We also thank the patients who volunteered to participate in this study. *Conflict of Interest*: None declared.

Address correspondence to Daniel Yoshor, Department of Neurosurgery, Baylor College of Medicine, One Baylor Plaza, S-603, Houston, TX 77030, USA. Email: dyoshor@bcm.edu.

References

Allison T, Begleiter A, McCarthy G, Roessler E, Nobre AC, Spencer DD. 1993. Electrophysiological studies of color processing in human visual cortex. Electroencephalogr Clin Neurophysiol. 88:343–355.

Allison T, Ginter H, McCarthy G, Nobre AC, Puce A, Luby M, Spencer DD. 1994. Face recognition in human extrastriate cortex. J Neurophysiol. 71:821–825.

Allison T, McCarthy G, Nobre A, Puce A, Belger A. 1994. Human extrastriate visual cortex and the perception of faces, words, numbers, and colors. Cereb Cortex. 4:544–554.

Allison T, Puce A, Spencer DD, McCarthy G. 1999. Electrophysiological studies of human face perception. I: Potentials generated in occipitotemporal cortex by face and non-face stimuli. Cereb Cortex. 9:415–430.

Allman J, Miezin F, McGuinness E. 1985. Stimulus specific responses from beyond the classical receptive field: neurophysiological mechanisms for local-global comparisons in visual neurons. Annu Rev Neurosci. 8:407–430.
Annese J, Gazzaniga MS, Toga AW. 2005. Localization of the human cortical visual area MT based on computer aided histological analysis. Cereb Cortex. 15:1044–1053.
Arroyo S, Lesser RP, Poon WT, Webber WR, Gordon B. 1997. Neuronal generators of visual evoked potentials in humans: visual processing in the human cortex. Epilepsia. 38:600–610.
Brewer AA, Liu J, Wade AR, Wandell BA. 2005. Visual field maps and stimulus selectivity in human ventral occipital cortex. Nat Neurosci. 8:1102–1109.
Cavonius CR, Hilz R. 1973. Invariance of visual receptive-field size and visual acuity with viewing distance. J Opt Soc Am. 63:929–933.
Curatolo JM, Macdonell RA, Berkovic SF, Fabinyi GC. 2000. Intraoperative monitoring to preserve central visual fields during occipital corticectomy for epilepsy. J Clin Neurosci. 7:234–237.
Dagnelie G, Spekreijse H, van Dijk B. 1989. Topography and homogeneity of monkey V1 studied through subdurally recorded pattern-evoked potentials. Vis Neurosci. 3:509–525.
DeYoe EA, Carman GJ, Bandettini P, Glickman S, Wieser J, Cox R, Miller D, Neitz J. 1996. Mapping striate and extrastriate visual areas in human cerebral cortex. Proc Natl Acad Sci USA. 93:2382–2386.
DiCarlo JJ, Maunsell JH. 2003. Anterior inferotemporal neurons of monkeys engaged in object recognition can be highly sensitive to object retinal position. J Neurophysiol. 89:3264–3278.
Dougherty RF, Koch VM, Brewer AA, Fischer B, Modersitzki J, Wandell BA. 2003. Visual field representations and locations of visual areas V1/2/3 in human visual cortex. J Vis. 3:586–598.
Dow BM, Snyder AZ, Vautin RG, Bauer R. 1981. Magnification factor and receptive field size in foveal striate cortex of the monkey. Exp Brain Res. 44:213–228.
Dumoulin SO, Bittar RG, Kabani NJ, Baker CL Jr, Le Goualher G, Bruce Pike G, Evans AC. 2000. A new anatomical landmark for reliable identification of human area V5/MT: a quantitative analysis of sulcal patterning. Cereb Cortex. 10:454–463.
Efron B. 1982. The jackknife, the bootstrap, and other resampling plans. Philadelphia, PA: Society for Industrial Mathematics.
Engel AK, Moll CK, Fried I, Ojemann GA. 2005. Invasive recordings from the human brain: clinical insights and beyond. Nat Rev Neurosci. 6:35–47.
Engel SA, Glover GH, Wandell BA. 1997. Retinotopic organization in human visual cortex and the spatial precision of functional MRI. Cereb Cortex. 7:181–192.
Fried I, MacDonald KA, Wilson CL. 1997. Single neuron activity in human hippocampus and amygdala during recognition of faces and objects. Neuron. 18:753–765.
Gallant JL, Shoup RE, Mazer JA. 2000. A human extrastriate area functionally homologous to macaque V4. Neuron. 27:227–235.
Gonzalez F, Relova JL, Prieto A, Peleteiro M. 2005. Evidence of basal temporo-occipital cortex involvement in stereoscopic vision in humans: a study with subdural electrode recordings. Cereb Cortex. 15:117–122.
Grill-Spector K, Kourtzi Z, Kanwisher N. 2001. The lateral occipital complex and its role in object recognition. Vision Res. 41:1409–1422.
Grill-Spector K, Malach R. 2004. The human visual cortex. Annu Rev Neurosci. 27:649–677.
Halgren E, Baudena P, Heit G, Clarke JM, Marinkovic K, Clarke M. 1994. Spatio-temporal stages in face and word processing. I. Depth-recorded potentials in the human occipital, temporal and parietal lobes [corrected]. J Physiol Paris. 88:1–50.
Haxby JV, Gobbini MI, Furey ML, Ishai A, Schouten JL, Pietrini P. 2001. Distributed and overlapping representations of faces and objects in ventral temporal cortex. Science. 293:2425–2430.
Horton JC, Hoyt WF. 1991. The representation of the visual field in human striate cortex. A revision of the classic Holmes map. Arch Ophthalmol. 109:816–824.
Huettel SA, McKeown MJ, Song AW, Hart S, Spencer DD, Allison T, McCarthy G. 2004. Linking hemodynamic and electrophysiological measures of brain activity: evidence from functional MRI and intracranial field potentials. Cereb Cortex. 14:165–173.
Huk AC, Dougherty RF, Heeger DJ. 2002. Retinotopy and functional subdivision of human areas MT and MST. J Neurosci. 22:7195–7205.
Ishai A, Ungerleider LG, Martin A, Haxby JV. 2000. The representation of objects in the human occipital and temporal cortex. J Cogn Neurosci. 12(Suppl 2):35–51.
Kastner S, De Weerd P, Pinsk MA, Elizondo MI, Desimone R, Ungerleider LG. 2001. Modulation of sensory suppression: implications for receptive field sizes in the human visual cortex. J Neurophysiol. 86:1398–1411.
Kawano K, Shidara M, Watanabe Y, Yamane S. 1994. Neural activity in cortical area MST of alert monkey during ocular following responses. J Neurophysiol. 71:2305–2324.
Kreiman G, Fried I, Koch C. 2002. Single-neuron correlates of subjective vision in the human medial temporal lobe. Proc Natl Acad Sci USA. 99:8378–8383.
Kreiman G, Koch C, Fried I. 2000. Imagery neurons in the human brain. Nature. 408:357–361.
Marg E, Adams JE, Rutkin B. 1968. Receptive fields of cells in the human visual cortex. Experientia. 24:348–350.
Maunsell JH. 1995. The brain's visual world: representation of visual targets in cerebral cortex. Science. 270:764–769.
Maunsell JH, Van Essen DC. 1983. Functional properties of neurons in middle temporal visual area of the macaque monkey. II. Binocular interactions and sensitivity to binocular disparity. J Neurophysiol. 49:1148–1167.
Noachtar S, Hashimoto T, Luders H. 1993. Pattern visual evoked potentials recorded from human occipital cortex with chronic subdural electrodes. Electroencephalogr Clin Neurophysiol. 88:435–446.
Quiroga RQ, Reddy L, Kreiman G, Koch C, Fried I. 2005. Invariant visual representation by single neurons in the human brain. Nature. 435:1102–1107.
Rolls ET, Tovee MJ. 1995. The responses of single neurons in the temporal visual cortical areas of the macaque when more than one stimulus is present in the receptive field. Exp Brain Res. 103:409–420.
Schmolesky MT, Wang Y, Hanes DP, Thompson KG, Leutgeb S, Schall JD, Leventhal AG. 1998. Signal timing across the macaque visual system. J Neurophysiol. 79:3272–3278.
Schulder M, Holodny A, Liu WC, Gray A, Lange G, Carmel PW. 1999. Functional magnetic resonance image-guided surgery of tumors in or near the primary visual cortex. Stereotact Funct Neurosurg. 73:31–36.
Sereno MI, Dale AM, Reppas JB, Kwong KK, Belliveau JW, Brady TJ, Rosen BR, Tootell RB. 1995. Borders of multiple visual areas in humans revealed by functional magnetic resonance imaging. Science. 268: 889–893.
Sereno MI, Tootell RB. 2005. From monkeys to humans: what do we now know about brain homologies? Curr Opin Neurobiol. 15:135–144.
Smith AT, Singh KD, Williams AL, Greenlee MW. 2001. Estimating receptive field size from fMRI data in human striate and extrastriate visual cortex. Cereb Cortex. 11:1182–1190.
Spiridon M, Fischl B, Kanwisher N. 2006. Location and spatial profile of category-specific regions in human extrastriate cortex. Hum Brain Mapp. 27:77–89.
Tootell RB, Dale AM, Sereno MI, Malach R. 1996. New images from human visual cortex. Trends Neurosci. 19:481–489.
Tootell RB, Hadjikhani N. 2001. Where is 'dorsal V4' in human visual cortex? Retinotopic, topographic and functional evidence. Cereb Cortex. 11:298–311.
Tootell RB, Tsao D, Vanduffel W. 2003. Neuroimaging weighs in: humans meet macaques in "primate" visual cortex. J Neurosci. 23:3981–3989.
Van Essen DC. 2004. Towards a quantitative, probabilistic neuroanatomy of cerebral cortex. Cortex. 40:211–212.
Van Essen DC, Drury HA. 1997. Structural and functional analyses of human cerebral cortex using a surface-based atlas. J Neurosci. 17: 7079–7102.
Van Essen DC, Newsome WT, Maunsell JH. 1984. The visual field representation in striate cortex of the macaque monkey: asymmetries, anisotropies, and individual variability. Vision Res. 24:429–448.
Wilson CL, Babb TL, Halgren E, Crandall PH. 1983. Visual receptive fields and response properties of neurons in human temporal lobe and visual pathways. Brain. 106(Pt 2):473–502.